Enhanced Critical Currents of Superconducting $ErNi_2B_2C$ in the Ferromagnetically Ordered State

P. L. Gammel, B. Barber, D. Lopez, A. P. Ramirez, and D. J. Bishop
Bell Laboratories, Lucent Technologies, Murray Hill, New Jersey 07974

S. L. Bud'ko and P. C. Canfield
Ames Laboratory and Department of Physics and Astronomy, Iowa State University, Ames, Iowa 50011
(Received 7 June 1999)

We report on transport and magnetization studies of the critical current in single crystal $ErNi_2B_2C$ for applied fields below 4 kG. Below $T \approx 2.5$ K superconductivity coexists with weak ferromagnetism. We find that the critical currents are strongly enhanced for all field orientations in this ferromagnetic regime, corresponding to a threefold increase of the pinning force of the flux line lattice. We speculate that this increase is due to strong pair breaking by the ferromagnetism.

PACS numbers: 74.60.Jg, 74.60.Ge, 74.70.Dd

Local moment magnetic order and superconductivity have conventionally been thought to be antagonistic ground states. However, over the last 20 years the discovery of a number of magnetic superconductors has allowed for a better understanding of how magnetic order and superconductivity can indeed coexist [1]. In particular, starting with the $(RE)Rh_4B_4$ and $(RE)Mo_6(S/Se)_8$ and culminating with $(RE)Ni_2B_2C$ [2,3], where (RE) is a rare earth, it has been repeatedly shown that antiferromagnetism readily coexists with type II superconductivity. In the $(RE)Ni_2B_2C$ system it has even been seen [4] that magnetic structures can couple directly to superconductivity via the flux line lattice (FLL) structures for (RE) = *Tm*, as manifest by a shared magnetic state and FLL phase diagram.

Historically, the coexistence of ferromagnetism and superconductivity has been a much trickier negotiation. In the case of $ErRh_4B_4$, for example, once the Er sublattice starts to order ferromagnetically, superconductivity exists for only approximately 0.1 K below the Curie temperature [1]. On the other hand, in addition to superconductivity coexisting with both the paramagnetic and antiferromagnetically ordered (RE) sublattice of the $(RE)Ni_2B_2C$ compounds, magnetization data suggest that weak ferromagnetism (WFM) and superconductivity coexist for (RE) = Er below $T \sim 2.5$ K. Upon cooling the local moment sublattice in $ErNi_2B_2C$, like that in $TbNi_2B_2C$, has an initial transition from the paramagnetic state to an antiferromagnetically ordered state [5,6], followed at lower temperatures by a transition to an ordered state with a net ferromagnetic component to the ordered moment [6,7]. The primary difference between $ErNi_2B_2C$ and $TbNi_2B_2C$ is that for RE = Er there is a superconducting transition at $T_c = 10$ K above both of the magnetic ordering temperatures, $T_N = 6$ K and $T_{\mathrm{WFM}} \approx 2.5$ K. The initial speculation [7] about this WFM state in $ErNi_2B_2C$ has now been confirmed: As in the case of $TbNi_2B_2C$, spin-polarized neutron diffraction [8] and ancillary supporting data [9,10] detect a net ordered moment below T_{WFM}. Prior to the decisive spin-polarized neutron diffraction studies, our experimental search for binary, ternary, and quaternary second phases in $ErNi_2B_2C$ failed to identify any which order ferromagnetically near 2.5 K, adding further supporting evidence that the ferromagnetism is intrinsic. The details of the state in which weak ferromagnetism and superconductivity coexist are much less clear, although several possibilities have been described. One exciting prospect is a spontaneously generated FLL in zero applied magnetic field [11]. Certainly this system will be forced to develop new and interesting states in response to this coexistence.

In this paper we report on a series of magnetization and transport measurements on $ErNi_2B_2C$. Like all other superconducting members of the $(RE)Ni_2B_2C$ series, $ErNi_2B_2C$ has a Ginzburg-Landau parameter $\kappa \geq 5$, implying that the superconducting properties are controlled by the FLL. In particular, we focus on the phase below $T_{\mathrm{WFM}} \approx 2.5$ K, where weak ferromagnetism and superconductivity coexist. We show that ferromagnetism enhances both the vortex pinning and critical currents in this type II superconductor. We speculate that the ferromagnetism arises from ordering of the sharp domain walls within the incommensurate modulation, with wave vector $q = 0.553a^*$, of the highly anisotropic Er local moments below 6 K. Further, locally strong pair breaking at a domain wall is the origin of the enhanced pinning.

The experiments described here were performed on high quality single crystals from batches grown using isotopically enriched ^{11}B to minimize the absorption of thermal neutrons used in the separate FLL imaging experiments [12,13]. The data presented here are of two types. The first are magnetization studies taken with a quantum design SQUID magnetometer with the field applied along the [100], [110], and [001] crystallographic directions of as grown crystals. The isothermal $M(H)$ loops were taken after zero-field cooling (ZFC) the sample to the chosen temperature and then cycling from $H = 0$ up to $+55$ kG, then down to -55 kG, and finally back to 0: i.e., the data do not include the virgin curve. The second type of data

are from transport measurements of the critical current using $1 \times 1 \times 5$ mm^3 bars cut from the larger crystals with one short dimension along [001] and the long dimension along [100] or [110]. For these transport measurements, the sample was first etched using HF followed by aqua regia to reduce surface pinning and then contacted using Pt wires and Epotek-H20E silver epoxy, yielding contact resistances of $<1\ \Omega$. The critical current was obtained by regulating the dc current through the sample with a feedback loop. The feedback signal was derived from a fixed, low frequency, ac current summed with the dc, and the loop was designed to keep the ac component of the voltage across the sample fixed as a function of field or temperature. Typically the ac component was fixed at 1 μV, although the trends in the data presented were insensitive to this exact value.

Shown in Fig. 1 are representative magnetization data for the field along [110]. Much more extensive data sets along both [110] and [100] follow the same trends illustrated here. In the lower panel are M-H loops at a variety of temperatures spanning T_{WFM}. Above 1500 G, one clearly sees the feature that led to the speculation [7] of weak ferromagnetism in this system. For $T > 2.5$ K, and M-H loops extrapolate to near zero at $H = 0$, after accounting for the diamagnetism due to the superconductivity. Below 2.5 K, the extrapolation, indicated by the dashed line, becomes nonzero, saturating at $\sim 0.3\mu_B$/Er for $T < 2$ K and following a temperature dependence reminiscent of a developing order parameter. A heuristic argument for this moment has been given in terms of the domain walls in the antiferromagnetic state as follows. The Er spins are approximated by a four position clock model [14] with a saturated moment of $9\mu_B$/Er. The wave vector of the incommensurate modulation of $0.553a^*$

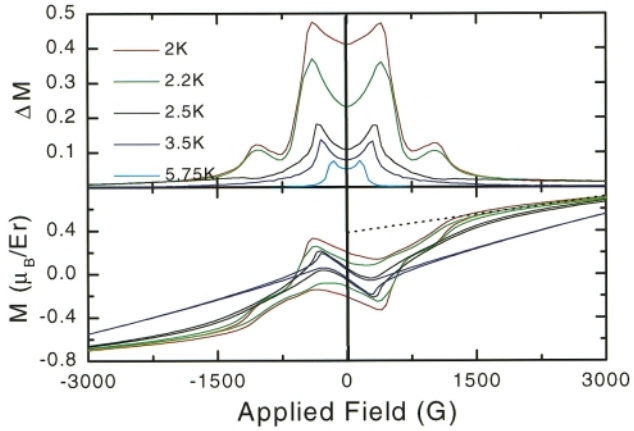

FIG. 1 (color). Shown (bottom panel) are M-H loops at different temperatures for fields $H \parallel [110]$. The dotted line is the extrapolation used to suggest the development of a ferromagnetic moment $\sim 0.3\mu_B$/Er below $T_{\mathrm{WFM}} \approx 2.5$ K. In the upper panel the hysteresis $\Delta M \sim I_c$ in the M-H loops is shown as a function of temperature. Below $T_{\mathrm{WFM}} \approx 2.5$ K the hysteresis increases dramatically, and a second feature near ~ 1200 G develops. Data for fields $H \parallel [100]$ are generically similar.

can be interpreted as a simple nearest neighbor antiferromagnet with a ferromagnetic domain wall (two aligned spins) every $(0.553 - \frac{1}{2})a^* \sim 70$ Å. Intense higher order harmonics in the neutron diffraction have been used to argue for the sharpness of these domain walls [15]. While there are many possibilities for the ordering within the ferromagnetic state, a rough estimate for the magnitude of the ordered moment can be derived assuming the domain walls order ferromagnetically. In this case, a net moment $\sim 9(0.053) \sim 0.4\mu_B$/Er ensues, similar to what is seen in the data.

In addition to this extrapolation it is clear from the M-H loops that substantial additional hysteresis develops below 2.5 K. In the top panel of Fig. 1 we show the hysteresis $\Delta M = |M_{\mathrm{up}} - M_{\mathrm{down}}|$ as a function of temperature. Several features are evident. First, there is a dramatic overall increase in ΔM below T_{WFM}. Second, the position of the first maximum increases from ~ 300 G to ~ 500 G. This feature, which roughly coincides with the minimum in the initial ZFC M-H, is often taken as a measure of H_{cl}. It is unclear if this increase below T_{WFM} is related to H_{cl}, or somehow involves extra terms from the coercive field of the ferromagnetic state. Third, a second maximum in ΔM appears near 1200 G for $T < T_{\mathrm{WFM}}$.

In a nonmagnetic superconductor, the hysteresis in the M-H loops is related to the critical current using the familiar Bean model [16] as $\Delta M \propto I_c$. The data of Fig. 1 can then be used to construct the temperature dependence of I_c for different applied field directions. In Fig. 2 the zero-field value of ΔM is plotted. These data are extracted from hysteresis loops with H along the three unique crystallographic directions: [100], [110], and [001]. The increase in ΔM for $T < T_{\mathrm{WFM}}$ is most clearly seen for H applied along the [110]. Similar, albeit less pronounced, increases in ΔM can be seen for the field along other directions. Comparable increases in ΔM are found for all fields below $H = 4000$ G with the most distinct increases found for fields near the local maxima in ΔM. Based on these data there appears to be a dramatic increase in I_c for temperatures below T_{WFM}.

In a magnetic superconductor, and, in particular, in a ferromagnetically ordered state, the validity of the Bean model for constructing the critical current can be questioned. For example, if there is a coercive field associated with the magnetism, then the hysteresis in the M-H loops below the coercive field will contain contributions from both the superconducting critical currents and magnetic hysteresis. Preliminary SANS data with $H \parallel a$ show that for field cooled experiments with $H > 500$ G, $B \sim H$ and B is carried by the vortex lattice, justifying our qualitative use of the Bean model and allowing us to consider constructs, such as the pinning force, used in nonmagnetic superconductors.

To verify and expand upon our interpretation of the magnetization data, we have also measured the transport critical current as described above for samples

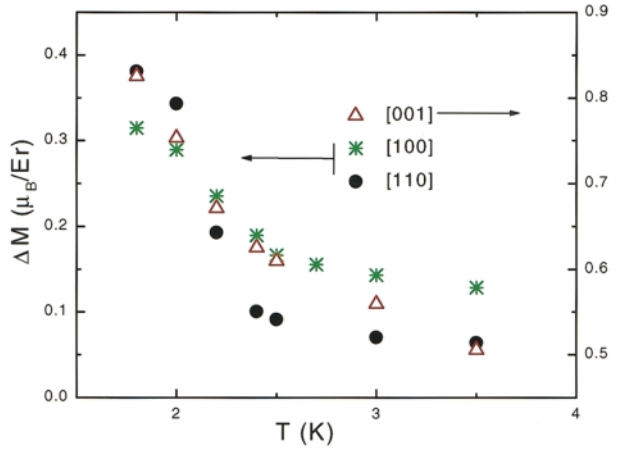

FIG. 2 (color). Relative magnetization critical currents $\Delta M \sim I_c$ at zero applied field as a function of temperature for three different field orientations. Data at other applied fields are similar. The data for $H \parallel [110]$ are taken from the data of Fig. 1. The rapid increase below $T_{\mathrm{WFM}} \sim 2.5$ K is most pronounced for $H \parallel [110]$. Note: The data for $H \parallel [001]$ plotted against the right axis have an offset zero.

immersed in liquid helium. The data (shown in the lower panel of Fig. 3) were taken as temperature sweeps at fixed field following a field cooled process

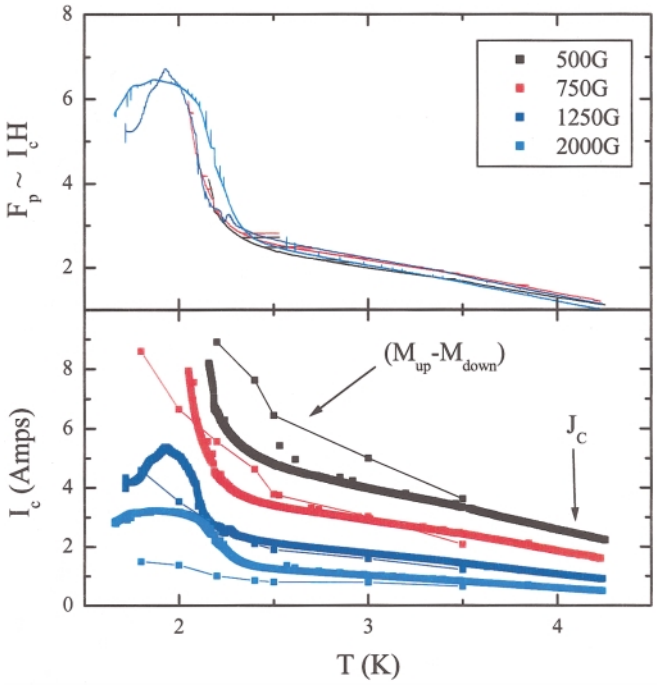

FIG. 3 (color). Shown (bottom panel) are the transport critical currents for fields applied along [001] and current along [100]. Also included are the magnetization critical currents for the same fields, scaled to match the transport data at 3.5 K and 500 G. Even in this orientation, perpendicular to the developing ferromagnetic moment, there is a pronounced increase in I_c below $T_{\mathrm{WFM}} \approx 2.5$ K. In the upper panel, a plot of the pinning force $F_P \sim I_c H$ improves the scaling of the data and shows a roughly threefold increase.

for the magnetic field applied along [001] and current along [100]. For currents above 8 A, self-heating of the samples set in, so we were able to explore only a limited temperature range at the lowest applied fields. Also plotted in the lower panel of Fig. 3 are the magnetization critical currents, scaled to match the transport data at 500 G and 3.5 K. This scaling coincides with estimates of the magnetization critical current from the Bean model. Generally, and similar to the magnetization data, there is a pronounced increase in the critical currents below T_{WFM}, although the data sets are different in detail. It should be noted that for $H \parallel [010]$ the transport data (not shown) showed no sign of the second peak near 1200 G in the magnetization data. We now believe the second peak is associated with a low field metamagnetic transition in the ordered sublattice. This underscores the need to measure both I_c and ΔM in a magnetic superconductor.

To attempt to understand the origin of this increase, the pinning force on the flux lines $F_P \propto I_c H$ is plotted in the upper panel of Fig. 3. Data with the field along [010] were generically similar. For $T > T_{\mathrm{WFM}}$, this shows that the critical current data roughly scale with the pinning force. Although outside the scope of this Letter, it is worth commenting that the pinning force for $T > T_{\mathrm{WFM}}$ is roughly linear and extrapolates to zero for $T \sim T_N$. This is consistent with the large changes in bulk pinning in the incommensurately ordered phase reported earlier [17].

Scaling of the magnetization critical currents using the pinning force was similar, but showed breakdown of the scaling at low fields ($<$1000 G). The increase in the pinning force can be ascribed to enhanced pair breaking associated with the ferromagnetic order [18], although without detailed knowledge of the ordered state it is difficult to get a quantitative comparison with our data. Within the heuristic model of the ferromagnetic moment resulting from local aligned moments at the domain walls, we anticipate that this local ferromagnetism will have the same strong pair breaking as a ferromagnetic impurity. Similarly, the peak in I_c near T_{WFM} is expected due to enhancing pair breaking from critical fluctuations [13,19]. Overall, the transport and magnetization give a consistent picture of the increase in critical current below T_{WFM}.

Over the years, a number of workers have used ferromagnetic impurities, with their concomitant strong pair breaking, as pinning centers to increase the critical current in superconducting samples, and, in particular, superconducting wires [20]. One difficulty of interpreting the specific role of ferromagnetism in those data is that for the impurities used ferromagnetism sets in at a much higher temperature than superconductivity, i.e., $T_{\mathrm{FM}}(\mathrm{impurity}) \gg T_c(\mathrm{bulk})$. In such a case it is hard to make the case that ferromagnetism is important as opposed to the mere presence of impurities and defects in the host structure. In $ErNi_2B_2C$ there are two clear advantages in studying the effects of ferromagnetism on superconducting critical current. First and foremost is that $T_{\mathrm{WFM}}(\mathrm{bulk}) < T_c(\mathrm{bulk})$,

so one can unambiguously see the effect that magnetic order has on pinning and the critical current through studies above and below T_{WFM}. Second, in $ErNi_2B_2C$ the ferromagnetism is intrinsic [7,8] to the material, so the issue of boundary and surface effects is not present.

Our previous small angle neutron scattering (SANS) measurements [12] of the FLL with the magnetic field applied along the c axis in $ErNi_2B_2C$ suggested that there is a coupling of the FLL to the ferromagnetism in this system. The SANS data measure the longitudinal correlation length ξ_L, the distance over which the flux lines are correlated parallel to the applied field. Within models of weak, random pinning ξ_L is inversely proportional to I_c [12]. The SANS data show several surprising effects. The first is that ξ_L is roughly field independent over the studied range. This is in stark contrast to what is expected and seen in conventional superconductors in which, as the field is increased, the FLL interaction energy increasingly dominates over the pinning energy and all correlation lengths increase. The explanation for this is that the domain walls in the incommensurate antiferromagnetic state provide a cutoff in space for how long the correlations can grow, causing ξ_L to saturate. The second observation is that at roughly 2.5 K the longitudinal correlation length rapidly drops, indicating that below this temperature the lattice is strongly disordered. This effect mirrors the increase in I_c described here and can hence be attributed to increased pairbreaking and pinning associated with the ferromagnetic state. The final observation from SANS studies relevant to our discussion is that at this same temperature, the flux lines are seen to rotate away from the applied field direction by as much as 1°. This suggests the development of an in-plane component to the magnetization. This moment is from the basal plane ferromagnetism, and its addition as a vector sum to the applied field causes a rotation of the direction of the FLL. The scaling of these rotations was discussed in a recent theoretical paper [21].

The observation that ferromagetic regions can effectively pin vortex lines opens up the possibility of many novel types of devices and experiments. For normal types of flux line pinning, the pinning force is only weakly field dependent. The effectiveness of the pinning depends on field because the interaction energy changes relative to the pinning energy making the lattice either easier to harder to pin. For the type of pinning demonstrated here, the interaction between a single flux line and a pinning center can be field dependent. Therefore one can envisage building devices where the strength of the pinning is field tunable. For example, one could use a transverse magnetic field to change the vortex behavior in the plane and build latching devices and magnetic switches. One can imagine devices in which there is low pinning to allow field lines to enter the sample and then the pinning is increased, holding a well-ordered lattice in place. There are many nonequilibrium dynamic states that can also be formed with such a field tunable pinning site and many new structures remain to be discovered.

In conclusion, we have presented both magnetization and transport data on the magnetic superconductor $ErNi_2B_2C$. Below 2.5 K, there is a transition into a state with coexistence of superconductivity and weak ferromagnetism with an ordered moment in the plane of $\sim 0.3\mu_B/\mathrm{Er}$. Our measurements of the critical current of this type II superconductor show that, contrary to intuition, not only can ferromagnetism and superconductivity coexist, but the onset of ferromagnetic order increases the critical current of this system. Clearly, the interplay of superconductivity and magnetism is a rich and interesting source of new physics that holds many surprises in store for us.

[1] Ø. Fisher, in *Ferromagnetic Materials*, edited by K. Buschow and E. Wolfarth (Elsevier, Amsterdam, 1990), Vol. 5, Chap. 6.
[2] R. J. Cava *et al.*, Nature (London) **367**, 254 (1994).
[3] P. C. Canfield, P. L. Gammel, and D. J. Bishop, Phys. Today **51**, No. 10, 40–46 (1998).
[4] M. R. Eskildsen *et al.*, Nature (London) **393**, 242 (1998).
[5] B. K. Cho *et al.*, Phys. Rev. B **52**, 3684 (1995).
[6] B. K. Cho, P. C. Canfield, and D. C. Johnston, Phys. Rev. B **53**, 8499 (1996).
[7] P. C. Canfield, S. L. Bud'ko, and B. K. Cho, Physica (Amsterdam) **262C**, 249 (1996).
[8] H. Kawano *et al.*, J. Phys. Chem Solids **60**, 1053 (1999).
[9] P. Dervenagas *et al.*, Phys. Rev. B **53**, 8506 (1996).
[10] D. R. Sanchez *et al.*, Phys. Rev. B **57**, 10 268 (1998).
[11] T. K. Ng and C. M. Varma, Phys. Rev. Lett. **78**, 330 (1997).
[12] U. Yaron *et al.*, Nature (London) **382**, 236 (1996).
[13] P. L. Gammel *et al.*, Phys. Rev. Lett. **82**, 1756 (1999).
[14] P. C. Canfield *et al.*, Phys. Rev. B **55**, 970 (1997); P. C. Canfield and S. L. Bod'ko, J. Alloys Compd. **262/263**, 169 (1997).
[15] J. Zaretsky *et al.*, Phys. Rev. B **51**, 678 (1995); S. K. Sinha *et al.*, Phys. Rev. B **51**, 681 (1995).
[16] M. Tinkham, *Introduction to Superconductivity* (Krieger, Malabar, FL, 1980), pp. 173ff.
[17] C. D. Dewhurst *et al.*, Phys. Rev. Lett. **82**, 827 (1999).
[18] K. Maki in *Superconductivity*, edited by R. D. Parks (Marcel Dekker, New York, 1969), pp. 1036–1105.
[19] T. V. Ramakrishnan and C. M. Varma, Phys. Rev. B **24**, 137 (1981).
[20] N. D. Rizzo *et al.*, Appl. Phys. Lett. **69**, 2285 (1996); T. H. Alder and J. D. Livingston, J. Appl. Phys. **37**, 3551 (1966).
[21] T. K. Ng and C. M. Varma, Phys. Rev. Lett. **78**, 3745 (1997).